Inhibition of Mitochondrial Fission by Drp-1 Blockade by Short-Term Leptin and Mdivi-1 Treatment Improves White Adipose Tissue Abnormalities in Obesity and Diabetes

P Finocchietto, H Perez, G Blanco, Miksztowicz, C Marotte, C Morales, J Peralta, G Berg, C Poderoso, JJ Poderoso, MC Carreras

PII: S1043-6618(21)00612-5

DOI: https://doi.org/10.1016/j.phrs.2021.106028

Reference: YPHRS106028

To appear in: *Pharmacological Research*

Received date: 24 August 2021
Revised date: 25 November 2021
Accepted date: 6 December 2021

Please cite this article as: P Finocchietto, H Perez, G Blanco, Miksztowicz, C Marotte, C Morales, J Peralta, G Berg, C Poderoso, JJ Poderoso and MC Carreras, Inhibition of Mitochondrial Fission by Drp-1 Blockade by Short-Term Leptin and Mdivi-1 Treatment Improves White Adipose Tissue Abnormalities in Obesity and Diabetes, *Pharmacological Research,* (2021) doi:https://doi.org/10.1016/j.phrs.2021.106028

Inhibition of Mitochondrial Fission by Drp-1 Blockade by Short-Term Leptin and Mdivi-1 Treatment Improves White Adipose Tissue Abnormalities in Obesity and Diabetes

Finocchietto P [1,2], Perez H [1], Blanco G [3], Miksztowicz V [4,5], Marotte C[1], Morales C [6], Peralta J [1,2], Berg G[5], Poderoso C[7], Poderoso JJ [1], Carreras MC [1]

[1]Laboratorio de Metabolismo del Oxígeno INIGEM-UBA-CONICET, Buenos Aires, Argentina

[2]Departamento de Medicina, Facultad de Medicina, Universidad de Buenos Aires, Buenos Aires, Argentina

[3]Laboratorio de Inmunotoxicología (LaITo), IDEHU-CONICET, Universidad de Buenos Aires

[4]Facultad de Medicina, Pontificia Universidad Católica Argentina (UCA), Instituto de Investigaciones Biomédicas (UCA-CONICET), Laboratorio de Patología Cardiovascular Experimental e Hipertensión Arterial, Buenos Aires, Argentina.

[5]Laboratorio de Lípidos y Aterosclerosis, Departamento de Bioquímica Clínica, Facultad de Farmacia y Bioquímica, Instituto de Fisiopatología y Bioquímica Clínica (INFIBIOC), Universidad de Buenos Aires, Buenos Aires, Argentina.

[6]Departamento de Patología, Facultad de Medicina. Instituto de Fisiopatología Cardiovascular, Universidad de Buenos Aires

[7]Departamento de Bioquímica Humana, Facultad de Medicina, Universidad de Buenos Aires

*Corresponding author: Paola Finocchietto, Laboratorio de Metabolismo del Oxígeno INIGEM-UBA-CONICET, Departamento de Medicina, Facultad de Medicina, Universidad de Buenos Aires. Córdoba Av. 2351 (C 1120 AAR), Buenos Aires, Argentina. Tel./Fax +54115950-8365, +5411554153012

E-mail: pfinocchietto@gmail.com

Abstract

Background.

Obesity and type 2 diabetes are chronic diseases characterized by insulin resistance, mitochondrial dysfunction and morphological abnormalities. **Objective**. We have investigated if dysregulation of mitochondrial dynamics and biogenesis is involved in an animal model of obesity and diabetes.

Methods.

The effect of short-term leptin and mdivi-1 –a selective inhibitor of Drp-1 fission-protein– treatment on mitochondrial dynamics and biogenesis was evaluated in epididymal white adipose tissue (WAT) from male *ob/ob* mice.

Results.

An increase in Drp-1 protein levels and a decrease in Mfn2 and OPA-1 protein expression were observed with enhanced and sustained mitochondrial fragmentation in *ob/ob* mice compared to *wt C57BL/6* animals ($p<0.05$). The content of mitochondrial DNA and PGC-1α mRNA expression –both parameters of mitochondrial biogenesis– were reduced in *ob/ob* mice ($p<0.05$). Treatment with leptin and mdivi-1 significantly increased mitochondrial biogenesis, improved fusion-to-fission balance and attenuated mitochondrial dysfunction, thus inducing white-to-beige adipocyte transdifferentiation. Measurements of glucose and lipid oxidation in adipocytes revealed that both leptin and mdivi-1 increase substrates oxidation while *in vivo* determination of blood glucose concentration showed decreased levels by 50% in *ob/ob* mice, almost to the *wt* level.

Conclusions.

Pharmacological targeting of Drp-1 fission protein may be a potential novel therapeutic tool for obesity and type 2 diabetes.

Keywords:

white adipose tissue, mitochondria, biogenesis, dynamics, Drp-1, mdivi-1

Abbreviations Used

AMPK: AMP-dependent kinase

BAT: brown adipose tissue

DAF-FM: amino-5-methylamino-2¢,7¢-difluorofluorescein diacetate

DRP-1: dynamin-related protein-1

FFA: free fatty acid

LC3-II: microtubule-associated protein 1A/1B-light chain 3

Mdivi-1: selective inhibitor of Drp1

Mfn2: mitofusin proteins

NO: nitric oxide

NRF1: nuclear respiratory factor

Ob/ob: leptin-deficient mice

OPA-1: optic atrophy-1

OXPHOS: oxidative phosphorylation system

PE: phosphatidylethanolamine

PGC-1α: proliferator-activated receptor gamma coactivator-1 alpha

RNS: reactive nitrosative species

ROS: reactive oxygen species

RT-PCR, reverse transcription-polymerase chain reaction

siRNA: small interference RNA

UCP-1: uncoupler protein 1

WAT: white adipose tissue

INTRODUCTION

Obesity and type 2 diabetes are chronic diseases that typically coexist and have grown in prevalence to become a global health problem. Both of them share a pathophysiological axis of insulin resistance (IR), oxidative stress, mitochondrial dysfunction and chronic inflammation. Obesity is characterized by an abnormal increase in white adipose tissue (WAT) mass depicting an imbalance between energy intake and consumption that leads to energy overload (1,2).

In mammals, there are three types of adipose tissue: white, brown and beige, with distinct functions and morphology, different protein expression patterns, and dissimilar developmental origins (3,4). While the function of WAT is to store energy in the form of lipid droplets that can be released to fuel other tissues, brown adipose tissue (BAT) has thermogenic properties for maintaining body temperature (5-7). Browning is the process by which some adipocytes within WAT depots acquire properties of brown adipocytes (an increase in mitochondrial content and oxidative metabolism) showing an intermediate phenotype between white and brown adipocytes ("beige" or "brite") (8).

Leptin, the satiety and anti-obesity hormone, is an adipokine released from white fat tissue that acts on the hypothalamus to induce satiety and reduce food intake, and on the peripheral tissues to control metabolism and to increase the metabolic rate (9).*Ob/ob* mice suffer a mutation that determines a premature stop codon in the *Lep* gene (leptin) and constitute a well-known model of obesity and type 2 diabetes characterized by hyperglycemia, hyperinsulinemia, high food intake, mitochondrial dysfunction, and oxidative/nitrosative stress affecting mitochondrial complex I activity in WAT, liver and skeletal muscle (10,11).

Insulin resistance is a common characteristic of type 2 diabetes and obesity, with which mitochondrial dysfunction has been associated. Changes in shape or size of mitochondria have been observed in diabetic patients and animal models in which there is decreased mitochondrial fusion and elevated fission. Mitochondria from type 2 diabetic patients are smaller than in healthy controls, and hyperglycemia induce mitochondrial fragmentation in different cell types, including heart, liver, cardiovascular or pancreas. Exercise fosters an improvement in fat oxidation and insulin sensitivity, as well as a decrease in DRP1 and an increase of Mfn1/2 expression. (12).

Mitochondria are dynamic organelles essential for cellular energy survival and a major site of ROS production. These organelles, whose morphology has a remarkable plasticity according to the energetic cell needs, undergo constant mitochondrial fusion and fission, and are replaced every 2–4 weeks in different tissues through mitophagy. All of these processes are necessary for mitochondrial quality control and clearance (13,14). Energetic homeostasis is sustained through the balance among mitochondrial biogenesis, dynamics, ultrastructure, function and degradation in a healthy mitochondrial population (15). While mitochondrial fusion is mediated by the mitofusin proteins (Mfn) 1 and 2 in the outer membrane and by OPA-1 (optic atrophy-1) in the inner membrane, mitochondrial fission requires the translocation of Drp-1, a member of the large GTPases dynamic family, from the cytosol to the mitochondrial outer membrane. When the cytosolic protein Drp-1 is activated, it translocates to the outer membrane of the mitochondria where it multimerizes generating a ring-like structure that constricts and divides this organelle. Post-translational modifications of the protein contribute to the regulation of mitochondrial fission mainly by phosphorylation of serine residues that increase or decrease its GTPase activity (16). Drp-1 activation is rapidly regulated by the phosphorylation of serine 616 and dephosphorylation of serine

637, which are targeted by different phosphatases and kinases. While phosphorylation of Drp-1 on Ser-637 prevents its mitochondrial translocation, phosphorylation of Drp-1 on Ser-616 promotes mitochondrial fragmentation during mitosis (17,18).

Mdivi-1 is a quinazolinone that selectively inhibits Drp-1 over other dynamin family members and prevents mitochondrial fission by pharmacological inhibition. This drug inhibits Drp-1 self-assembly into rings and its association with mitochondria (19,20).

Mitochondrial biogenesis is the process through which new mitochondria are generated, driven by the transcriptional activators NRF-1 and 2 and by PGC-1α. It is activated by various signaling pathways, including nitric oxide (NO)/cyclic GMP, Akt and AMPK, among others (21). The AMP-activated protein kinase (AMPK) is a cellular energy sensor that under activation by phosphorylation leads to upregulation of PGC-1α, UCP-1, and mitochondrial biogenesis (22).

The development of compounds targeted at mitochondrial fusion, fission and mitophagy has exponentially gained interest in the last years, highlighting the importance of these targets for therapy against metabolic diseases. The oral antidiabetic drug. Metformin has demonstrated beneficial effects by protecting mitochondrial integrity through the inhibition of Drp-1 activity. Likewise, mdivi-1 can also improve insulin sensitivity in conditions of insulin resistance. Some authors have demonstrated that mdivi-1 reduces mitochondrial fragmentation, oxidative stress, inflammation and atherosclerosis, and improves endothelial function in diabetic mice (23-25).

In this context, the twofold aim of the present study is to investigate if dysregulation of mitochondrial dynamics and biogenesis are involved in a single model of obesity and diabetes, and if Drp-1 can be pharmacologically targeted as a potential novel therapeutic tool for obesity and diabetes.

MATERIALS AND METHODS

Animals experimentation.

Male *ob/ob* (± 70 g) and *wt C57BL/6* (± 25 g) 5-month-old mice were purchased from Jackson Labs (USA). Animal experiments were performed in accordance with the Principles of Laboratory Animal Care. The animal experiments were approved by the local Scientific and Technology Ethics Committee at the University of Buenos Aires (UBA). All efforts were made to minimize animal suffering and to reduce the number of animals used. Mice were maintained under controlled temperature (21º C +/- 2º C), humidity (50–60%), and air-flow conditions, with a fixed 12-h light/dark cycle. Until the experiment onset, all animals were fed with a standard mice laboratory chow and had free access to food and water to standardize their nutritional status. Animals were sacrificed by cervical dislocation at the end of the treatment with leptin or mdivi-1.

Drug administration.

Wt C57BL/6 and *ob/ob* mice received short-term (3 days) intraperitoneal injection of pyrogen-free dimethyl-sulfoxide, or recombinant leptin (1 mg/kg/d dissolved in dimethyl-sulfoxide) (L 3772 Sigma Chemical Co.), or mdivi-1 (50 mg/kg/d dissolved in dimethyl-sulfoxide) (Mdivi-1 MO199 Sigma Chemical Co). In all mice, body weight and food intake were measured (11,26).

Blood glucose determination.

On the day of sacrifice, blood samples were collected using cardiac puncture. Blood glucose concentration was determined by Accu-check performance glucometer (Roche Lab). Animals were fasted for 10h before the procedures.

White adipose tissue extraction. Mice were sacrificed by cervical dislocation and epididymal white adipose tissue (6-10 g) was immediately extracted and homogenized in sucrose buffer 20% (TRIS 10 mM, EDTA 0.1mM, sucrose 20%, 2% protease inhibitor cocktail) (Sigma Aldrich, St. Louis, MO, USA). The homogenate was centrifuged at 800*g* for 10 min at 4°C, frozen in liquid nitrogen and stored at 80ºC until further analysis (11,26).

Western Blot Analysis. Proteins (50 μg) were separated using electrophoresis on 7.5-10% SDS-polyacrylamide gel, and transferred to a PVDF membrane (GE, Healthcare). Membranes were incubated with antibodies against 1: 1000 anti-Mfn2 (H-68): sc-50331, 1: 4000 anti-actin (I- 19): sc-1616 obtained from Santa Cruz, CA or 1: 1000 anti-OPA-1: 612607 and 1: 1000 anti-Drp-1: 611113 obtained from BD Biosciences, 1:1000 anti-LC3 II (L7543 Sigma-Aldrich), 1: 1000 anti-phospho-Drp1 (Ser616): #3455, 1: 1000 anti-phospho-Drp1 (Ser637): #6319, 1:1000 anti-AMPKα: #2532, 1:1000 anti-phospho AMPKα (Thr172): #2531 obtained from Cell Signaling. After several washes, the membranes were incubated with appropriate horseradish peroxidase conjugated secondary antibodies. Detection of immunoreactive proteins was accomplished by enhanced chemiluminescence. Quantification of bands was performed by digital image analysis using Total Lab Analyzer software (Nonlinear Dynamics Ltd, Biodynamics, Argentina). Equal loading was controlled with the appropriate markers (11,26,27).

Electron microscopy images.

WAT was fixed in 4% paraformaldehyde, 2% glutaraldehyde, and 5% sucrose in PBS, followed by 2-h post-fixation in 1% osmium tetroxide, and then 1 h in uranyl acetate in 50% ethanol. Samples were washed with ethanol 50% and dehydrated with a graded series of ethanol, clarified with acetone and embedded in Vestopal. Grids were prepared

and stained with uranyl acetate and lead citrate. Samples were observed at 100 kV with a Zeiss EM-109-T transmission electron microscope (Zeiss, Oberkochen, Germany) (11,26,27).

Optic microscopy images and histological evaluation.

The histological examination by light microscopy was performed in a blinded manner. Fixed epididymal WAT samples were dehydrated in ethanol, embedded in paraffin wax, and cut with a microtome Reichert (Austria). The resulting micro-sections were stained with hematoxylin and eosin reagent and periodic acid-schiff (PAS) stain for the determination of size and density of adipocytes and vascular density. In both cases the quantification was performed at high power field (HPF), 20 fields at 400x magnification for each animal using a computerized image analyzer (Image Pro Plus, Media Cybernetics Corp) (28).

Isolation of mitochondria.

Mitochondria were isolated from homogenized WAT by differential centrifugation. Mitochondrial pellets were stored in the presence of antiproteases and antiphosphatases as described (11,26,27).

Mitochondrial complex I activity.

The activity of Complex I (NADH: ubiquinone reductase) was determined spectrophotometrically following the reduction of 50 μM 2,3-dimethoxy-6-methyl-1,4-benzoquinone at 340 nm by 50 μg/ml mitochondrial proteins with a Hitachi U3000 spectrophotometer at 30°C; 200 μM NADH was used as electron donor. Reaction was carried out in the presence of 1 mM KCN and expressed as nmol of reduced benzoquinone/min.mg prot. Complex I activity was selectively inhibited by 10 μM rotenone (11,26).

Primary fat cell isolation.

WAT pads were weighed and sliced into 3 mm pieces with scissors and resuspended in 5 ml of KRH buffer (25 mM $NaHCO_3$, 12 mM KH_2PO_4, 1.2 mM $MgSO_4$, 4.8 KCl, 120 mM NaCl, 1.4 mM $CaCl_2$, 5 mM glucose, 20 mM Hepes, 2% protease inhibitor cocktail (Sigma Aldrich, St. Louis, MO, USA), pH7.4, plus 2.5% BSA containing 0.5 mg/ml collagenase (Sigma Chemical Co., St Louis, MO, USA). The fat pads were digested for 45-60 minutes at 37ºC in an orbital bath shaking at 100 rpm. Adipocytes released from the tissue were harvested by centrifugation (400g, 15 min). Cells in the upper phase of the centrifuge tube were collected, washed three times and resuspended in 0.15 M PBS. Adipocytes were isolated from animals without treatment and under the different treatments (11).

Fluorescence microscopy images and analysis.

Adipocytes from mice under treatment were stained with mitotracker green (50uM) (Invitrogen Carlsbad, CA) and observed under an Olympus BX-51 fluorescence microscope equipped with a digital Q-Color 3 Olympus camera. Digital images were processed with Image-Pro Plus 6.0 software (Media Cybernetics, Rockville, MD, USA) and Cell Profiler (Broad Institute, USA). A Cell Profiler pipeline was created for the segmentation of individual mitochondria and measurement of morphometric parameters. Several images for each treatment were processed with this pipeline to identify and measure more than 300 mitochondria. All morphometric measurements of mitochondria were exported to a standard database and were further analyzed with Cell Profiler Analyst (Broad Institute, USA). A standard random forest classification algorithm was used to implement a machine learning approach to classify mitochondria intro three groups: round, elongated and branched. The training procedure was repeated until global classification accuracy achieved 90%, with 100% classification accuracy of

the round mitochondria subgroup. Then, the whole set was scored for the amount of mitochondria belonging to each of the three groups in percentage. We were able to introduce a morphological classification of mitochondria in three categories into a machine learning algorithm. In a training environment made of selected images from evidently round elongated and complex shape mitochondria, the algorithm incorporated several morphometric parameters as a set of rules to discriminate between the morphology of the three groups (supervised learning). The parameters selected by the algorithm included roundness (also known as form factor), minor axis length, minimum and maximum ferret diameter, compactness, and eccentricity among others. However, single statistical analyses of these parameters showed that none of them could discriminate between groups when assessed alone as a sole surrogate for mitochondrial shape change. This fact reinforces the concept that by combining several morphometric parameters in a set of rules, the supervised machine learning algorithm improved the ability to discriminate mitochondrial shape changes beyond that of single morphometric parameters (29-31).

Adipocytes siRNA transfection.

Adipocytes were transfected with siRNAsDrp-1 or empty-vector siRNA (Santa Cruz Biotechnology) 50nM using lipofectamine (Invitrogen Corp. California, USA) in Opti-MEM reduced serum medium and were incubated at 37ºC in 5% CO_2 for 10 hours, according to the protocol provided by the manufacturer (11). The sequence of siRNAs Drp-1-sc-45953 was designed on the structure of mice genome (11,26).

Oxidative metabolism in isolated adipocytes

Isolated adipocytes were incubated with leptin (200 ng/ml), mdivi-1 (50 uM) or siRNA Drp-1 (50nM) for 10h, and with [14C] palmitic acid, samples were distributed into tubes containing Whatman filter paper soaked in NaOH and 200 nCi/ml [14C] palmitic

acid. The tubes were sealed and incubated for 2 h; then, 10 N HCl was added to release [14C] CO, which was detected by scintillation counting of the filter paper. To measure complete glucose oxidation to CO_2 and H_2O, samples were supplemented with [14C] D-glucose [250 mCi/mmol]. Radioisotopes were from Perkin-Elmer Life and Analytical Sciences, Boston, MA, USA (11,26).

RNA Extraction and Real-Time PCR (RT-qPCR).

Total RNA was insulated from the different tissues using TriZol reagent following the manufacturer's instructions (Life Technologies, Inc.-BRL, Grand Island, NY). Any residual genomic DNA was removed by treating RNA with RQ1 Rnase-free DNase (Promega, Madison, WI, USA) at 37ºC for 30 min, which was subsequently inactivated by incubation with 2 mM EGTA for 10 min at 65°C. First-strand cDNA synthesis was performed using oligo(dT)18 primer, Invitrogen SuperScript IV Reverse Transcriptase (RT), and RNase inhibitor (RNasin, Promega, Madison, WI, USA). PCR amplification and analysis were performed with ABI PRISM 7500 Sequence Detector System (PE Applied Biosystems, Foster City, CA). SYBR Select Master Mix (Applied Biosystems, Carlsbad, CA, USA) was used for all reactions, following the manufacturer's instructions. Real-time PCR data were analyzed by calculating the $2^{-\Delta\Delta Ct}$ value (comparative Ct method) using GAPDH expression as housekeeping, performed in parallel as endogenous control (11,32,33). The primer sequences and the condition of each reaction are shown in Supplemental Table I.

mtDNA/nDNA ratio.

WAT was homogenized in lysis buffer (10 mM Tris-HCl pH 8,

1 mM EDTA, and 0.1% SDS). After adding proteinase K, lysates were incubated at 55°C for 3 h, vigorously vortexed and centrifuged (8,000 g for 15 min); the resting supernatant was vortexed with 1 ml protein precipitation solution (Gentra Puregene Kit)

for 30 sec and placed on ice for 5 min. The resulting supernatant was mixed with 1 volume of isopropanol and centrifuged (12,000 g for 15 min at 4°C) to precipitate DNA. The DNA pellets were washed with 70% ethanol, air dried, and dissolved in Tris-EDTA buffer. For mtDNA/nDNA qPCRs, 40 ng of total genomic DNA were used. The mtDNA/nDNA ratio was calculated using the formula: $2\times2^{(\Delta C_T)}$, where ΔC_T is the difference of C_T values between nDNA ß2M and the mtDNA 16S rRNA primers as shown in (32,33).

Statistical analysis

Data are presented as mean ± SEM according to the normal or skewed distribution. Significant differences between groups were accepted at $p < 0.05$. One-way ANOVA (multigroup comparisons) followed by Bonferroni's multiple comparison test or Dunnett's test were carried out with GraphPad Prism 5.01 (La Jolla, CA).

RESULTS

Short-term leptin and mdivi-1 treatment reverts mitochondrial morphological defects in WAT from *ob/ob* mice

Mitochondrial morphology defects were detected by TEM in WAT slices in *ob/ob* mice in comparison to *wt C57BL/6* and *ob/ob* treated with leptin or mdivi-1 mice. While *wt* mitochondria were predominantly tubular-shaped (80%), *ob/ob* mitochondria were aberrantly small and spherical in shape (85%) (Fig. 1 A and B). Leptin or mdivi-1 treatment resulted in a significant increase in tubular-shaped mitochondria (55% and 49%, respectively) (Fig. 1 C, D and E). As mitochondrial fragmentation and dysfunction lead to mitophagy, we analyzed WAT slices by TEM and observed mitochondria engulfed by double-membrane vacuoles with mitochondrial fragments indicating an active process of mitophagy in *ob/ob* mice (10 images per field). These

alterations were reduced after treatment with leptin (5 images per fields) or mdivi-1 (3 images per field) (Fig. 1F). Autophagosome formation was assessed by evaluating the conversion of the soluble form of microtubule-associated protein light chain 3 (LC3-I) to lipidated and autophagosome-associated form (LC3-II) by Western Blot of WAT homogenates. A significant increase in LC3-II/I in *ob/ob* was observed with a decrease of LC3II level and absence of LC3I in *ob/ob* treated animals (Fig. 1G). No changes were observed in *wt C57BL/6.*These results coincided with a higher number of mitochondria with alterations observed by electron microscopy suggesting abnormal mitochondrial recycling by mitophagy and mitochondrial biogenesis.

Short-term leptin and mdivi-1 treatment reverts mitochondrial morphological defects in isolated adipocytes from WAT

We investigated mitochondria morphological changes on isolated adipocytes from WAT *wt C57BL/6* or *ob/ob* mice treated with leptin or mdivi-1 intraperitoneally using a machine learning algorithm to allow automated classification of mitochondria shape into three groups: branched, round, or elongated, detected by fluorescence microscopy images (Suppl. Fig. 1 A).“Branched” mitochondria denoted complex shapes including T-shapes, Y-shapes, P-shapes, O-shapes, among others, and have been associated with particular bioenergetic profiles (29). The results of mitochondrial classification into each of the three groups through machine learning is shown in Fig. 2 A and B. The measurement confirmed that *ob/ob* mice had a higher percentage of round mitochondria compared to *wt C57BL/6* mice (46% to 18%), consistent with the TEM analysis in WAT slices. This percentage was partially restored in *ob/ob* mice treated with leptin (24%), and by mdvi-1 treatment (22%). The percentage of elongated mitochondria was strongly reduced in *ob/ob* mice when compared against *wt C57BL/6* mice (29% and 52%, respectively). Both leptin and mdivi-1 treatment increased the presence of

elongated mitochondria (39% and 38%, respectively). In contrast, *wt C57BL/6, ob/ob* and leptin-treated groups showed a similar percentage of branched mitochondria (29%, 24% and 26%, respectively), while mdivi-1-treated mice showed an increased proportion of branched mitochondria (43%). (Fig. 2B and Suppl. Fig. 1A). No changes were found in *wt C57BL/6* under any treatment.

Short-term leptin and mdivi-1 treatment modulates the protein levels related with mitochondria fission/fusion process in WAT from *ob/ob* mice

We examined if leptin can modulate mitochondria fission in leptin-deficient *ob/ob* mice with mitochondrial dynamics impaired and we analyzed the expression of the mitochondrial fission (Drp-1) protein in WAT with and without leptin treatment. Drp-1 protein level is increased by ~50% in the WAT of *ob/ob* mice compared to *wild type* animals (Fig. 3A). Drp1 activity is regulated by the opposing effects of phosphorylation at two key serine residues: phosphorylation of Ser 616 increases Drp-1 activity whereas it is decreased by phosphorylation of Ser 637 (34). We measured the phosphorylation of both residues and found an increase in p-Ser 616-Drp-1 (active form) whereas p-Ser 637-Drp-1 (inactive form) decreased in *ob/ob* mice (Fig. 3 B and C). Administration of leptin reverted the changes in Drp-1 expression and phosphorylation forms in *ob/ob* mice stimulating the Drp-1 inactive form (Figs. 3 A-C). In addition, we studied the effect of leptin and mdivi-1 on Mfn2 and OPA-1 fusion proteins levels, and observed a reduction in these protein levels in *ob/ob,* which were restored after treatment (Fig. 3 D and E). No significant changes were observed in wt C57BL/6 under any treatment.

Leptin and mdivi-1 increase the expression of PGC-1α and AMPK-P as well the mitochondrial mass in WAT from *ob/ob* mice

To determine the effect of leptin or mdivi-1 treatment in mitochondrial biogenesis, we assessed PGC-1α gene expression and mtDNA content. The mRNA level of PGC-1α

was significantly lower in *ob/ob* mice compared to *wt C57BL/6,* leptin or mdivi-1 treatment (Fig 4 A). mtDNA content showed a reduction in *ob/ob* mice compared to *wt C57BL/6*. Inhibition of Drp-1 by mdvi-1 and leptin led to increased mtDNA content (Fig. 4 B). WAT obtained from *ob/ob* mice revealed that AMPK expression was devoid in its phosphorylated form (active) as compared to *wt*, while leptin or mdivi-1 treatment increased AMPK-P protein expression (Fig. 4 C and D).

Drp-1 inhibition increases the oxidative metabolism and mitochondrial function in WAT isolated adipocytes from *ob/ob* mice

To study the [14C] palmitic acid and [14C] D-glucose oxidation *in vitro,* isolated adipocytes from *wt C57BL/6* and *ob/ob* mice were incubated with leptin, mdivi-1 or siRNADrp-1. Basal palmitic acid oxidation in adipocytes from *ob/ob* was ~20% of the *wt* (Fig. 5 A). Leptin, mdivi-1 and siRNADrp-1 significantly increased glucose oxidation in *ob/ob* (20 nmol/min./mg.protein, 22 nmol/min./mg.protein, and 26 nmol/min./mg.protein, respectively) compared to *ob/ob* basal level (5.4 nmol/min./mg.protein) (Fig 5 A). Likewise, leptin, mdivi-1 and siRNADrp-1 significantly increased palmitic acid oxidation in *ob/ob* (3.8 pmol/min./mg.protein, 3.3 pmol/min./mg.protein, and 2.5 pmol/min./mg.protein, respectively) compared to *ob/ob* basal level (1.5 pmol/min./mg.protein) (Fig. 5 B).

The activity of the mitochondrial electron transport chain (ETC) complex I was evaluated in mitochondria. An impairment of mitochondrial function was observed in *ob/ob* (-50%), while leptin, mdivi-1 and siRNADrp-1 caused a 5-fold increase (Fig. 5 C).

Leptin and mdvi-1 stimulate the "browning" process in WAT from *ob/ob* mice

In order to study whether the leptin or mdvi-1 treatments in *ob/ob* mice stimulate the "browning" process in WAT, we measured the adipocyte area, vascular density and

mRNA UCP-1 expression. We observed that leptin and mdivi-1 treatment reduced the adipocyte area while increased the vascular density (Fig. 6 A and B) and mRNA UCP-1 expression in *ob/ob* WAT (Fig. 6 C).

Effect of leptin and mdvi-1 in blood glucose level, body weight and food intake

Both leptin and mdivi-1 decreased the blood glucose concentration by 50% in *ob/ob* mice almost to the *wt* level. We did not observe any changes in body weight and food intake over the course of the treatments (Table 1).

DISCUSSION

We studied mitochondrial dynamics in *ob/ob* mice and *wt* in WAT, and assessed the pharmacological potential of Drp-1 inhibition for the treatment of diabetes and obesity. Our results show a decrease in mitochondrial size, and higher fragmentation and mitophagy in WAT of *ob/ob* mice compared to *wt*, that correlates with a decrease in Mfn2 and OPA-1 fusion proteins and an increase in Drp-1 fission protein and activation, suggesting an imbalance between fusion and fission processes.

In agreement with our data, evidence supports alterations in mitochondrial dynamics in high-fat-diet-fed dietary (HFD) mice with hyperleptinemic state. At the end of the HFD exposure, Mfn1/2 and OPA1 gene expression was found to be significantly reduced in mice exposed to the HFD compared to controls, while Drp-1 gene expression analyses revealed increased levels of mRNA in WAT from mice receiving the HFD (35).

Mitochondrial morphology and the bioenergetic status of the cell are closely linked to protein modifications related to the fission/fusion process. Elongated and “branched” mitochondria have been previously associated with improved OXPHOS and several bioenergetic advantages, while round mitochondria have been associated with a predominance of mitochondrial fission, increased mitophagy and poor bioenergetic performance (36). Drp1- deficiency results in unusually shaped, large mitochondria and

mdivi-1 treated animals showed a significant improvement in the fraction of elongated mitochondria with tubular mitochondria bent to self-fusion and forming a donut shape (37,38).

According to that, to confirm matching changes of mitochondrial morphology in cells, we studied the effect of leptin or mdvi-1 in isolated adipocytes from treated mice and observed an increment of elongated and branched mitochondria and a reduction of rounded mitochondria.

The activation of AMPK and the expression of PGC-1α -master regulators of mitochondrial biogenesis are reduced in *ob/ob* mice. Interestingly, treatment with Drp-1 inhibitor or with leptin (that restores Mfn2, OPA1 and Drp-1 levels) improves mitochondrial biogenesis in *ob/ob* mice. In addition to PGC-1α, a set of coordinated factors are required to stimulate mitochondrial biogenesis such as AMPK, nuclear respiratory factor NRF-1/2, oxidative stress, nitric oxide levels, and mitochondrial bioenergetic state. AMPK plays a role in mitochondrial homeostasis phosphorylating PGC-1α on specific serine and threonine residues leading to increased mitochondrial gene expression. It has also been reported that AMPK activation indirectly phosphorylates Drp-1 at Ser 637, and this phosphorylation has been linked to the inhibition of Drp-1 and a decrease in mitochondrial fission. In addition, AMPK and aerobic exercise downregulate the phosphorylation level of Drp-1 at Ser 616 which is upregulated by ROS. AMPK is activated by leptin in the peripheral tissues increasing fatty acid oxidation and glucose uptake. Leptin produces Drp-1 inhibition modulating mitochondrial fission and PGC-1α stimulation favoring mitochondrial biogenesis; both are protective effects mediated by AMPK (39,40).

Inhibition of Drp-1 in isolated adipocytes by leptin, mdivi-1 and siDRP-1 resulted in glucose and palmitic acid oxidation, and increased mitochondrial complex I activity in *ob/ob* mice. This is supportive of the notion that mitochondrial fusion is associated with the use of glucose as fuel versus diminished fusion enabling the utilization of glucose for lipogenesis. In both obesity and common forms of type 2 diabetes, glucose oxidation and storage are reduced, in parallel with reduced activity of the tricarboxylic acid cycle, b-oxidation, and electron transport enzymes, especially complex I with reductions in mitochondrial area and number (41). The balance of the relative activities of Mfn2 and Drp-1 appears to be the major determinant of the continuous remodeling of the mitochondrial reticulum, and manipulations of the levels of Mfn2 have been shown to alter expression of mitochondrial respiratory chain complexes. The deletion of Mfn1/2 resulted in mitochondrial fragmentation and a deleterious effect on mitochondrial oxygen consumption. The suppression of the electron transport chain (ETC) function was associated with reduced oxygen consumption with substrates for complexes I, III, and IV (42). A suppression of OPA-1 expression mirrored these results suggesting a global effect in decreasing energy production in the inhibition of mitochondrial fusion. Fusion inhibition correlated with a widespread loss of the membrane potential, supportive of a role for morphology affecting ETC function (43).

We also studied whether epididymal white adipose tissue would be capable of undergoing the browning process. The adipocytes termed “beige” or “brite” (brown in white) show an intermediate phenotype between white and brown adipocytes, exhibiting multilocular morphology, high metabolic rates, levels of mitochondrial content, levels of UCP-1 expression and vascularization (44,45). Our results show that inhibition of Drp-1 and the increase of Mfn2 fusion expression by leptin and mdivi-1 stimulate UCP-1 expression, reduce the adipocyte area and increase vascularization in *ob/ob* WAT. Our

results are in line with evidence that leptin and Mfn2 stimulate UCP-1 in WAT. A decrease in energy expenditure, an increase in lipogenesis, low levels of UCP-1 in BAT and an increment in circular shaped mitochondria has been shown in WAT and BAT of Mfn2-KO mice (46). Mitochondrial biogenesis and upregulating mitochondrial enzymes involved in the respiratory chain, and specific uncoupling proteins such as UCP-1 have demonstrated that mitochondrial homoeostasis plays a key role in morphological and molecular characteristic maintenance of adipocyte browning. A decrease in the mitochondrial number is tightly coupled with the beige-to-white adipocyte transition (47,48).

In accordance with the metabolic and mitochondrial effects, leptin and mdivi-1 treatment produce a significant decrease in blood glucose levels in *ob/ob* mice which typically exhibit high levels of blood glucose concentration. Normalization of blood glucose levels was not accompanied by a decrease in body weight and food intake, suggesting that blood glucose concentration was related to increased glucose oxidative metabolism secondary to changes in mitochondrial homeostasis.

Our study has potential limitations and further research is needed. We studied the AMPK / PGC-1α pathway related to mitochondrial dynamics and biogenesis in one animal model of obesity and type 2 diabetes. The effects of mdvi-1 on mitochondrial function in WAT should be studied in other models of metabolic disorders, insulin resistance and T2DM, and more metabolic parameters -such as oxidative stress, nitric oxide levels, and mitochondrial bioenergetic state- should be analyzed to correlate with mitochondrial homeostasis and the glucose and fatty acid oxidation pathway.

In summary, mitochondrial dysfunction has been related with obesity, insulin resistance and type 2 diabetes. It is known that obesity, a high fat diet and/or sedentary life style improve oxidative stress impairing the TCA cycle function leading to mitochondrial

fission, while exercise or calorie restriction improve the whole-body metabolism through mitochondrial turn over and expansion. To delve into these observations, we studied *ob/ob* obese mice, a model of leptin deficiency with hyperinsulinemia, reduced levels of AMPK-P and high levels of mitochondrial fission and mitophagy that induce mitochondrial dysfunction and increase oxidative and nitrosative stress in WAT.

The inhibition of mitochondrial fission by leptin and mdvi-1 stimulates mitochondrial biogenesis, fusion and oxidative capacity. Modulation of the mitochondrial network through Drp-1, a critical mediator of mitochondrial fission, would have an important role in browning white adipose tissue into beige adipocytes. We suggest that Drp-1 blocking can be now proposed as a novel therapeutic target for obesity and diabetes.

Acknowledgments

The authors would like to thank Margarita López, Fabiana Confente and Mariana López Ravasio for electron microphotographs, Inés Rebagliatta and Silvia Holod for technical support, Natalia Riobó for revising the manuscript; and Natalia Lupori for revising the English version.

Funding

This work was supported by Agencia Nacional de Promoción Científica y Tecnológica (FONCyT) grant, PICT 1781 and Universidad de Buenos Aires grant, UBACyT 20020130100574BA (to M.C.C.).

Duality of Interest.

No potential conflicts of interest relevant to this article were reported.

Author Contribution

P.F., M.C.C., and J.J.P. designed the study; P.F. performed experiments; H.P. performed the RNA extraction, Quantitative Real-Time PCR, and mtDNA content

experiment; G.B. performed fluorescence microscope experiment, V.M. and G.B. performed optic microscope and area, density and vascular white adipose tissue study, C.M. performed technical assistant, C.M. performed histological study, P.F., and M.C.C. collected and analyzed data; P.F., H.P., J.P., C.P., J.J.P. and M.C.C. wrote the manuscript.

REFERENCES

1-Leitner DR, Frühbeck G, Yumuk V, Schindler K, Micic D, Woodward E, and Toplak H. (2017). Obesity and Type 2 Diabetes**:** Two Diseases with a Need for Combined Treatment Strategies - EASO Can Lead the Way. Obes Facts. 10(5):483-492.

2-Boden G (2011). Obesity, insulin resistance and free fatty acids. Curr. Opin. Endocrinol. Diabetes Obes. 18:139–143.

3-Hildebran S, Stumer J, Pfeifer A (2018). PVAT and its relation to brown, beige and white adipose tissue in development and function. Front. Physiol.9:70.

4-Pfeifer A, and Hoffmann, LS (2015). Brown, beige,and white:the new color code of fat and its pharmacological implications. Annu. Rev. Pharmacol. Toxicol. 55, 207–227. doi: 10.1146/annurev-pharmtox-010814-124346.

5-Chusyd DE, Wang D, Huffman DM and Nagy TR (2016). Relationships between Rodent White Adipose Fat Pads and Human White Adipose Fat Depots. Front. Nutr. 3:10.

6-Smith SR, Lovejoy JC, Greenway F, Ryan D, de Jonge L, de la Bretonne J, et al. (2001). Contributions of total body fat, abdominal subcutaneous adipose tissue compartments, and visceral adipose tissue to the metabolic complications of obesity. Metabolism, 50(4):425–35.

7- Neeland IJ, Ayers CR, Rohatgi AK, Turer AT, Berry JD, Das SR, et al. (2013).

Associations of Visceral and Abdominal Subcutaneous Adipose Tissue with Markers of Cardiac and Metabolic Risk in Obese Adults. Obesity 21, E439-E447.

8-ChenY, Pan R, Pfeifer A (2017). Regulation of brown and beige fat by microRNAs. Pharmacol. Ther. 170, 1–7.

9-Pelleymounter MA, Cullen MJ, Baker MB, Hecht R, Winter D, Boone T, Collins F (1995). Effects of the obese Gene Product on Body Weight Regulation in ob/ob Mice. Science. 269:540-543.

10- Lindström P (2007). The Physiology of Obese-Hyperglycemic Mice [*ob/ob* Mice]. The Scientific World Journal. 7, 666–685.

11-Finocchietto P, Holod S, Barreyro F, Peralta JG, Alippe Y, Giovambattista G, Carreras MC, Poderoso JJ (2011). Defective Leptin-AMPK Pathway Induces NO Release and Causes Mitochondrial Dysfunction and Obesity in ob/ob Mice. Antioxidants & Redox Signaling. 15: 2395-406.

12- Rovira-Llopis S, Bañulsa C, Diaz-Morales N, Hernandez-Mijaresa A, Rocha M, Victor VM. Mitochondrial dynamics in type 2 diabetes: Pathophysiological implications Redox Biology 11 (2017) 637–645.

13-Wanga J, Toanb S, Zhoua H (2020). Mitochondrial quality control in cardiac microvascular ischemia-reperfusion injury: New insights into the mechanisms and therapeutic potentials. Pharmacological Research. 156:104771.

14-Kotiadis VN, Duchen MR, and Osellame LD (2014). Mitochondrial quality control and communications with the nucleus are important in maintaining mitochondrial function and cell health. Biochim. Biophys. Acta. 1840:1254–65.

15-Westermann B. Mitochondrial fusion and fission in cell life and death (2010). Nature Rev Mol Cell Biol. 11: 872-84.

16-Chen H and Chan DC (2005). Emerging functions of mammalian mitochondrial fusion and fission. Hum Mol Genet 14: R283–R289.

17-Twig G, Shirihai OS (2011). The Interplay Between Mitochondrial Dynamics and Mitophagy. Antioxidants & Redox Signaling. 14, DOI: 10.1089/ars.2010.3779.

18- Feng ST, Wang ZZ, Yuan YH, Le Wang X, Sun HM, *et al.* (2020).Dynamin-related protein 1: A protein critical for mitochondrial fission, mitophagy, and neuronal death in Parkinson's disease. Pharmacol Res; 151: 104553.

19- Smith G and Gallo G (2017). To mdivi-1 or not to mdivi-1: Is that the question? Dev Neurobiol.77(11): 1260–68.

20- Manczak M, Kandimalla R, Yin X, Reddy PH. (2019). Mitochondrial division inhibitor 1 reduces dynamin-related protein 1 and mitochondrial fission activity. Human Molecular Genetics, 28,2: 177–199.

21- Whitaker RM, Corum D, Beeson CC, and Schnellmann RG (2016). Mitochondrial Biogenesis as a Pharmacological Target: A New Approach to Acute and Chronic Diseases. Annu Rev Pharmacol Toxicol.56:229-49.

22- Jager S, Handschin C, St-Pierre J, Spiegelman BM (2007). AMP-activated protein kinase (AMPK) action in skeletal muscle via direct phosphorylation of PGC-1alpha. Proc. Natl. Acad. Sci. USA.104:12017–12022.

23-Diaz-Morales N, Rovira-Llopis S, Bañuls C, Escribano-Lopez I, Marañon AM, Lopez-Domenech S, Orden S, Roldan-Torres I, Alvarez A, Veses S, Jover A, Rocha M, Hernandez-Mijares A, Victor VM (2016). Are Mitochondrial Fusion and Fission Impaired in Leukocytes of Type 2 Diabetic Patients?, Antioxid. Redox Signal. 25 (2) :108115.

24-Jheng, HF, Tsai, PJ, Guo SM, Kuo LH, Chang CS, Su IJ, Chang CR, Tsai YS. Mitochondrial fission contributes to mitochondrial dysfunction and insulin resistance in skeletal muscle, Mol. Cell Biol. 32 (2) (2012) 309–319.

25-Ouyang Z, Xie M, Zou H (2016). Metformin Suppresses Diabetes-Accelerated Atherosclerosis via the Inhibition of Drp1- Mediated Mitochondrial Fission, Diabetes. 66(1): 193–205.

26- Finocchietto P, Barreyro F, Holod S, Peralta J, Franco MC, Méndez C, Converso DP, Estévez A, Carreras MC, Poderoso JJ (2008). Control of Muscle Mitochondria by Insulin Entails Activation of Akt2-mtNOS Pathway: Implications for the Metabolic Syndrome. PLoS ONE. 3(3): e1749.

27-Gonzalez AS, Elguero ME, Finocchietto P, Holod S, Romorini L, Miriuka SG, Peralta JG, Poderoso JJ,Carreras MC (2014).Abnormal mitochondrial fusion – fission balance contributes to the progression of experimental sepsis. Free Radical Research.1–15.

28- Miksztowicz V, Morales C, Barchuk M, López G, Póveda R, Gelpi R, Schreier L, l Rubio M, Berg G (2017). Metalloproteinase 2 and 9 Activity Increase in Epicardial Adipose Tissue of Patients with Coronary Artery Disease. Curr Vasc Pharmacol.15(2):135-143.

29- Carpenter AE, Jones TR, Lamprecht MR, Clarke C, Kang IH, Friman O, *et al.* (2006). CellProfiler: image analysis software for identifying and quantifying cell phenotypes. Genome biology.**7**(10)**:** R100.

30- Jones TR, Kang IH, Wheeler DB, Lindquist RA, Papallo A, Sabatini DM, *et al.* (2008). Cell Profiler Analyst: data exploration and analysis software for complex image-based screens. BMC bioinformatics. 9: 482.

31- Jones TR, Carpenter AE, Lamprecht MR, Moffat J, Silver SJ, Grenier JK, *et al.* (2009).Scoring diverse cellular morphologies in image-based screens with iterative feedback and machine learning. Proceedings of the National Academy of Sciences of the United States of America. 106(6)**:** 1826-1831.

32-Venegas V, Wang J, Dimmock D, Wong LJ (2011). Real-Time Quantitative PCR Analysis of Mitochondrial DNA Content.Curr. Protoc. Hum. Genet. 68:19.7.1-19.7.12.

33- Perez, H Finocchietto,PV, Alippe Y, Rebagliati I, Elguero ME, Villalba N, Poderoso JJ, Carreras MC (2018). p66Shc Inactivation Modifies RNS Production, Regulates Sirt3 Activity, and Improves Mitochondrial Homeostasis, Delaying the Aging Process in Mouse Brain Oxidative Medicine and Cellular Longevity1-13.

34- Otera H, Shihara N, K Mihara K (2013). New insights into the function and regulation of mitochondrial fission. Biochimica et Biophysica Acte. 5 :1256-1268.

35-Mancini G, Pirruccio K, Yang X, Blucher M, Rodeheffer M (2019). Mitofusin 2 in Mature Adipocytes Controls Adiposity and Body Weight. Cell Reports 26, 2849–2858.

36-Galloway CA, Lee H, Yoon Y (2012). Mitochondrial morphology-emerging role in bioenergetics. Free radical biology & medicine. 53(12)**:** 2218-2228.

37-Otera H, Ishihara N,Mihara K (2013). New insights into the function and regulation of mitochondrial fission. Biochim et Biophys Acta 1833,5: 1256–1268.

38- Wu Q, Gao C, Wang H, Zhang X, Li Q et al. (2018). Int J Biochem Cell Biol 94:44-55.

39-Toyama EQ, Herzig S, Courchet J, Lewis Jr TL, Losón OC, Hellberg K, Young NP, Chen H, Polleux F, Chan DC, Shaw RJ (2016).AMP-activated protein kinase mediates mitochondrial fission in response to energy stress Science.15; 351(6270): 275–281.

40-Zorzano A, Liesa M, Sebastián D, Segalés J, and Palacín M (2010). Mitochondrial fusion proteins: dual regulators of morphology and metabolism. Semin Cell Dev Biol. 21: 566-74.

41- Rovira-Llopisa S, Bañulsa C , Diaz-Moralesa N, Hernandez-Mijaresa A, Rochaa M, Victor VM (2017).Mitochondrial dynamics in type 2 diabetes: Pathophysiological implications. Redox Biology; 11: 637–64.

42-Dietrich MO,WuLiu Z, Horvath TL (2013). Mitochondrial Dynamics Controlled by Mitofusins Regulate Agrp Neuronal Activity and Diet-Induced Obesity. Cell 155, 188–199.

43- Yoon Y, Galloway CA, Jhun BS, T. Mitochondrial Dynamics in Diabetes. Antioxid. Redox Signal. 14, 439–457.

44- Chusyd DE, Wang D, Huffman DH, Nagy TR (2016). Relationships between Rodent white Adipose Fat Pads and Human white Adipose Fat Depots. Front. Nutr. 3:10. doi: 10.3389/fnut.2016.00010.

45- Barbatelli G, Murano I, Madsen L, Hao Q, Jimenez M, Kristiansen K, Giacobino JP, De Matteis R & Cinti S (2010). The emergence of cold induced brown adipocytes in mouse white fat depots is determined predominantly by white to brown adipocyte transdifferentiation. American Journal of Physiology: Endocrinology and Metabolism. 298 E1244–E1253.

46- Boutant M, Kulkarni SS, Joffraud M, Ratajczak J, Valera-Alberni M, Combe R, Zorzano A, Cantó C. Mfn2 is critical for brown adipose tissue thermogenic function. EMBO J. 2017; 36:1543–1558.

47- Herz CT and Kiefer FW (2019). Adipose tissue browning in mice and humans. Journal of Endocrinology. 241, R97–R109.

48-Kaisanlahti A & Glumoff T (2019). Browning of white fat: agents and implications for beige adipose tissue to type 2 diabetes. Journal of Physiology and Biochemistry 75:1–10.

LEGENDS of the FIGURES

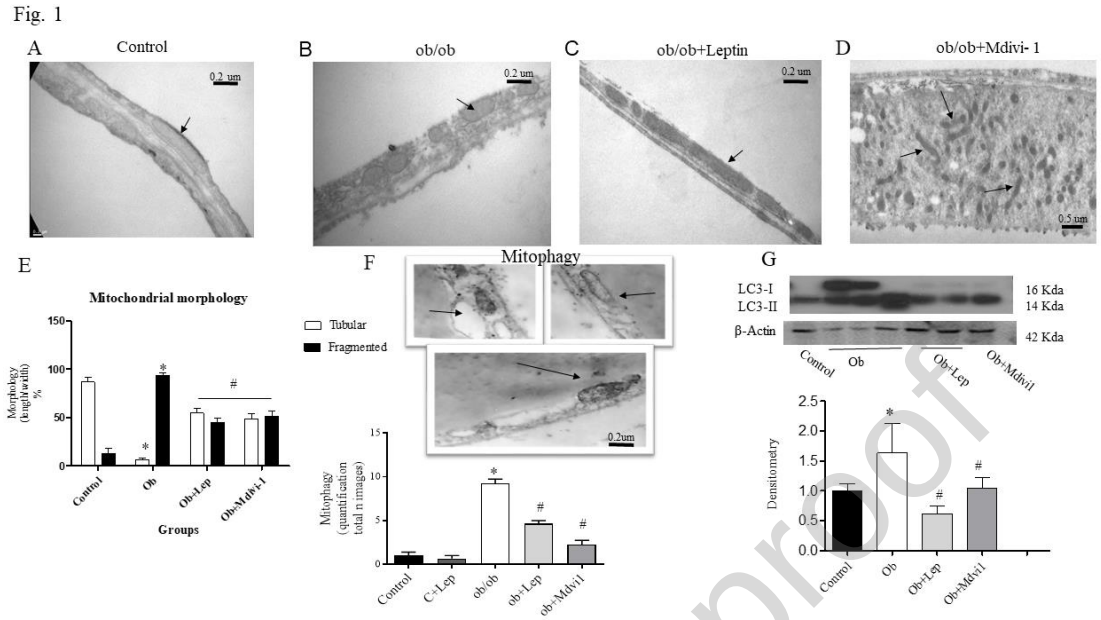

Figure 1- Effect of short-term leptin and mdivi-1 treatment on mitochondrial ultrastructural morphology Representative electron microscope images of mitochondrial morphology were evaluated using electron microscopy of fixed white adipose tissue from *wt C57BL/6* (A) or *ob/ob* (B) (Magnification 3000-30.000 X) with leptin (C), or mdivi-1(D) treatments (bar represents = micrometer), (5 images per animal for 6-8 per group) (black arrows). Tubular and fragmented mitochondria were counted per arbitrary area. (E) The percentage distribution of tubular and fragmented adipocyte mitochondria was determined in a minimum of 8–10 random fields at 3.000-30.000 X magnification to ensure a representative area of analysis. Those mitochondria whose length were more than thrice its width were considered tubular while round mitochondria were considered fragmented. (F) Representative images of WAT *ob/ob* mice slices reveal the presence of mitophagy characterized by autophagic vacuoles with mitochondrial particles or mitophagosomes (black arrows) (total images of mitophagy in 10 images per animals). (G) Representative Western blots of LC3 I/II protein. Bars reflect the densitometry in arbitrary units (A.U.) in absolute amount of protein. Data are

normalized to β-actin for protein. Results are mean ± SEM, n = 5-7, *p < 0.05 denotes different from respective *wt C57BL/6*. # p < 0.05 denotes different from respective, *ob/ob* vs *ob* + leptin or mdivi-1 treatment. n:5 per group.

Fig. 2

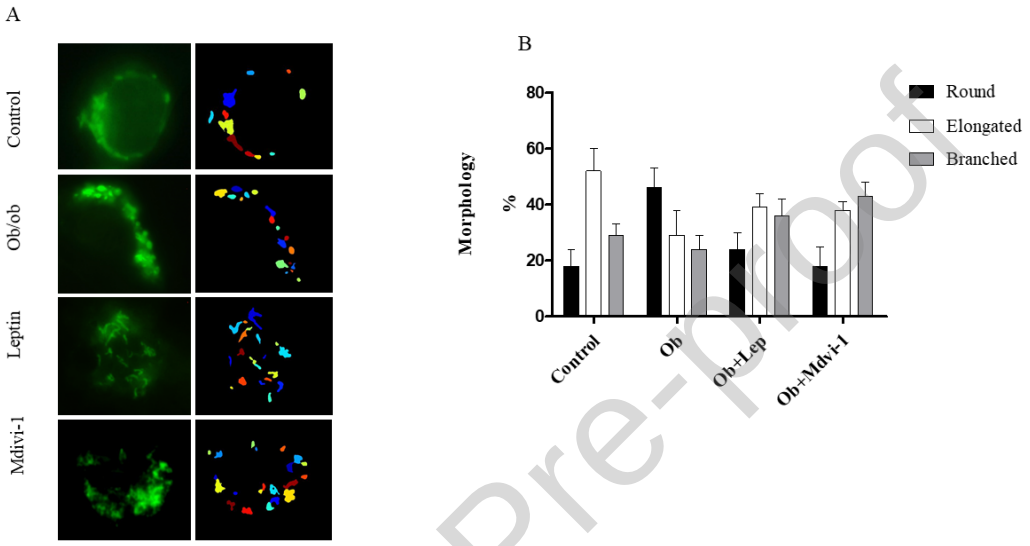

Figure 2- Effect of leptin and mdivi-1 on mitochondria shape-classes in adipocytes isolated from WAT, (A) Representative micrographs of adipocytes stained with mitotracker green and observed under fluorescence microscopy (digitally enlarged 1.000 x magnification), and their matching segmentation obtained with the Cell Profiler pipeline for extracting morphological measurements. Different mitochondrial colours mean mitochondrial morphology: blue and light blue: a branched, yellow: rounded, orange and red:elongated. (B) Proportions of the three defined mitochondria shape-classes among treatment groups with their corresponding 95% confidence intervals followed by supervised classification into three mitochondrial shape-classes (to further determine proportions of each class).

Fig. 3

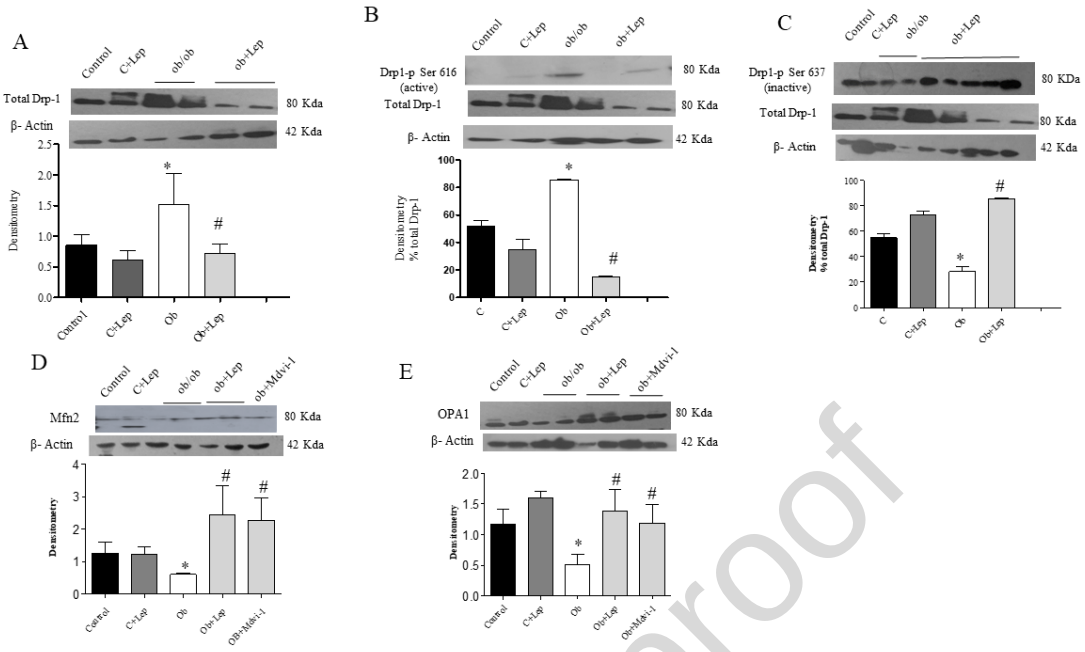

Figure 3- Effect of short-term leptin and mdivi-1 treatment on mitochondrial dynamics (A) Representative immunoblot of proteins separated using SDS-PAGE from whole WAT lysate reveals the protein of (A) Drp-1, (B) Drp-1 phosphorylated in Ser 616, bars reflect the Drp1-P protein quantified as a percentage of total Drp-1, (C) Drp-1 phosphorylated in Ser 637, bars reflect thep-Drp-1 protein quantified as a percentage of total Drp-1, and (D and E) the expression of fusion proteins Mfn2 and Opa-1. Data are normalized to β-actin for protein. Bars reflect the densitometry in arbitrary units (A.U.) in absolute amount of protein. *p < 0.05 denotes different from respective *wt C57BL/6*. # p < 0.05 denotes different from respective *ob/ob*, vs *ob* + leptin treatment (1 mg/kg i.p) and mdivi-1 (50mg/kg/d i.p). Results are mean ± SEM, n: 5-7 per group. One-way analysis of variance (ANOVA) and Bonferroni post hoc test.

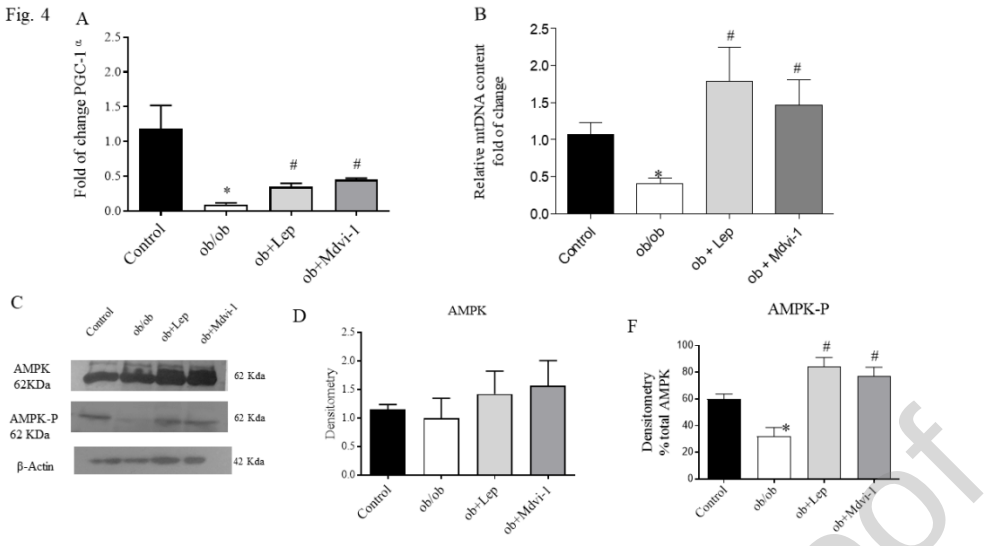

Figure 4- Effect of leptin and mdivi-1 on PGC-1α expression, mtDNA content and AMPK-P (A) The mRNA levels of PGC-1 α were measured in TRIZOL-treated WAT extracts from untreated wt C57BL/6 mice and *ob/ob* mice treated with leptin or mdvi-1.; GADPH mRNA was used as internal control and wt group measures were used as reference to compare between treatments. (B) Quantification of mtDNA and nuclear DNA content by qPCR in VAT in wt C57BL/6, *ob/ob* and *ob*+ leptin or mdvi-1 treatment, mtDNA/nDNA ratio was calculated ; ΔCT is the difference of CT values between nDNA ß2M and the mtDNA 16S rRNA primers and wt group measures were used as reference to compare between treatments (C) Representative immunoblot of proteins separated using SDS-PAGE from whole WAT lysate reveals the expression of AMPK and AMPK-P in wt, *ob/ob, ob* + leptin or mdvi-1. (D) Bars reflect the AMPK protein densitometry in arbitrary units (A.U.). (C) Bars reflect AMPK-P protein quantified as a percentage of total AMPK. Data are normalized to β-actin expression and wt group measures were used as endogenous control to compare between treatments. (Results are mean ± SEM, n: 6-7 per group. *p < 0.5 wt C57BL/6 vs *ob/ob*, # p < 0.05 *ob/ob* vs *ob* + leptin or mdvi-1. One-way analysis of variance (ANOVA) and Bonferroni post hoc test.

Fig. 5

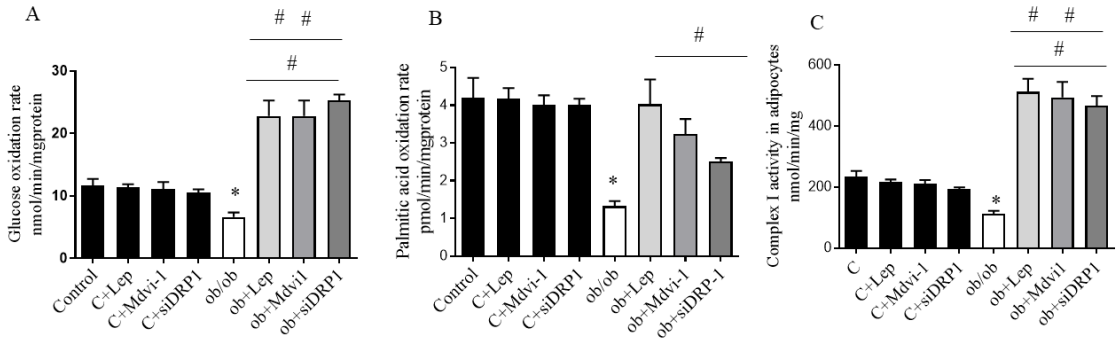

Figure 5- Effect of Drp-1 blocking on oxidative metabolism and mitochondrial function in isolated adipocytes from WAT

(A) Adipocytes from *wt* and *ob/ob* mice were isolated and incubated with leptin, mdivi-1 or siRNA Drp-1 and fat metabolism was measured as fatty acid oxidation with 1μCi/ml [14C]-palmitic acid oxidation to CO_2 and H_2O. Data resulted from pmolar/min./mg protein (Eli Wallac,;n= 5-6 per triplicate). (B) Glucose oxidation was measured with 1μCi/ml [14C]-D-glucose complete glucose oxidation to CO_2 and H_2O. Data resulted from nmolar/min./mg protein (Eli Wallac, n= 5-6 per triplicate). (C) Mitochondrial complex I activity was measured following the reduction of cytochrome c at 30 °C in the presence of NADH and KCN. The reaction rate was measured as the pseudo – first-order reaction constant (k ˈ) and expressed as k ˈ /min. mg protein. test. Results are mean ± SEM, n: 5-6 per group. * $p < 0.05$ *wt C57BL/6* vs *ob/ob,* # $p < 0.05$ *ob/ob* vs *ob*+ leptin or mdivi-1. One-way analysis of variance (ANOVA) and Bonferroni post hoc test. (D)Representative immunoblot of proteins separated using SDS-PAGE from whole WAT lysate reveals the expression of Drp-1 after transfection of *ob/ob* adipocytes with empty-vector and siRNA Drp-1 (50nM), respectively.

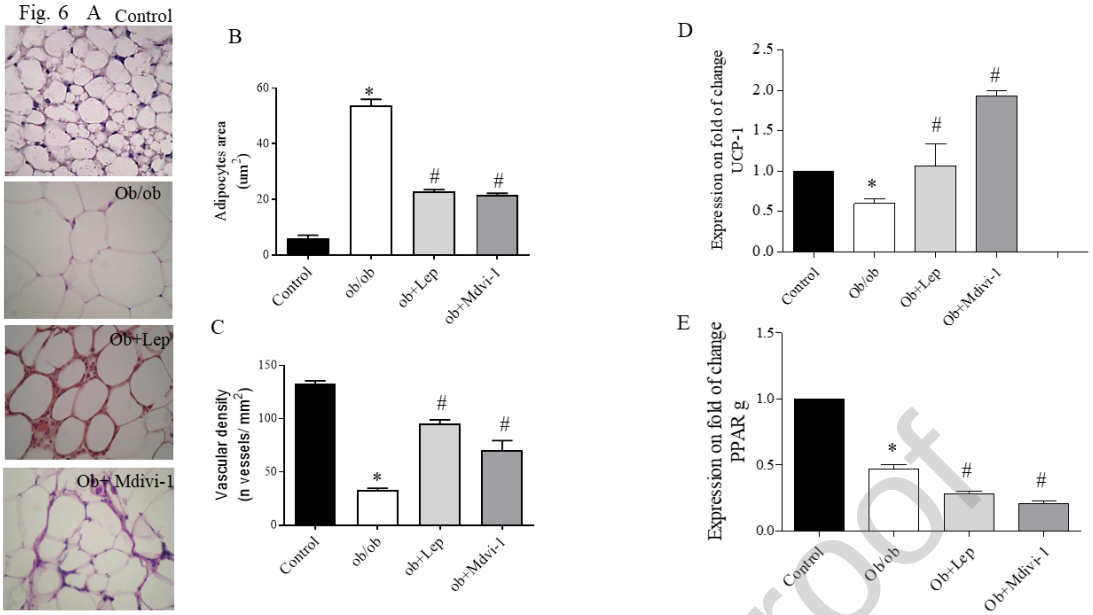

Figure 6- Effect of leptin and mdivi-1 on browning process on WAT

Representative micro-sections of WAT were stained with hematoxylin and eosin reagent and periodic acid-schiff (PAS) stain for studying the adipocytes area (B) and vascular density adipocyte (C) in all studied groups. (D) The mRNA levels of UCP-1 and (E) PPARγ were measured in Trizol-treated WAT extracts from all the studied groups; wt group were used as reference to compare between treatments. GADPH mRNA was used as internal control (n 5- 6). (Results are mean ± SEM, n: 6-7 per group. * $p < 0.05$ *wt* C57BL/6 vs *ob/ob*, # $p < 0.05$ *ob/ob* vs *ob* + leptin or mdivi- 1. One-way analysis of variance (ANOVA) and Bonferroni post hoc test.

Table 1: Effects of short-term leptin and mdivi-1 treatment on blood glucose levels, body weight and food intake

Variable	C	Ob/ob	Ob + Lep	Ob + Mdivi-1
Blood glucose levels (mg/ml)	138 ± 42	393 ± 36 *	198 ± 22 ≠	178 ± 35 ≠
Body Weight (g)	25 ± 4	70.6 ± 6 *	66 ± 4 *	65 ± 7 *
Food Intake (g/d)	2.4 ± 0.5	4.4 ± 0.4 *	3.8 ± 0.3*	3.5 ± 0.4*

(A) Blood glucose concentration (mg/dl) was measured in all studied groups. Body weight (g) and food intake (g/d) were determined in all animals during the study. Values are means ± SD of 8 mice per group *p<.0.5 *wt C57BL/6* vs *ob/ob*, #p < 0.05 *ob/ob* vs *ob* + leptin or mdivi-1. One-way analysis of variance (ANOVA) and Bonferroni post hoc.

SUPPLEMENTAL MATERIAL

Supplemental Table I. Mice gene-specific oligonucleotide sequences used in quantitative real-time polymerase chain reaction.

Gene	Primer sequence (5´to 3´)	Amplicon size (bp)	Annealing Temperature °C
PGC1-α Fw	GACCCTCCTCACACCAAACCC	149	60
PGC1-α Rv	TTTGGTGACTCTGGGGTCAGAG		
UCP-1 Fw	AGGCTTCCAGTACCATTAGGT	133	60
UCP-1 Rv	CTGAGTGAGGCAAAGCTGATTT		
GAPDH Fw	AGACAGCCGCATCTTCTTGT	148	62
GAPDH Rv	TGATGGCAACAATGTCCACT		
mtDNA 16S rRNA Fr	GCCTTCCCCCGTAAATGATA	97	62
mtDNA 16S rRNA R	TTATGCGATTACCGGGCTCT		
nDNA ß2M Fw	TGCTGTCTCCATGTTTGATGTATCT	86	62
nDNA ß2M Rev	TCTCTGCTCCCCACCTCTAAGT		

GADPDH, glyceraldehyde 3-phosphate dehydrogenase;

ß2M, β2-microglobulin

FW, forward; RV, reverse.

Supplemental Figure 1: Assessment of the fraction of mitochondria shape-classes by supervised classification

A Cell Profiler pipeline was created for the segmentation and measurement of morphometric parameters of individual mitochondria. Several images were processed with this pipeline for each treatment and morphometric parameters were exported and processed with Cell Profiler Analyst (Broad Institute, USA). A classification algorithm was used to implement a machine learning approach to classify mitochondria intro three groups: round, elongated and branched. The training procedure was repeated until global classification accuracy achieved 90%, with 100% classification accuracy of the round mitochondria subgroup (further details and references in methods section).

(A) An example of a supervised classification of a single image used to verify the ability to discriminate among morphological classes. Different mitochondrial colors mean mitochondrial morphology: blue and light blue: branched, yellow: rounded, orange and red: elongated.

(B) A sample of the training set used for machine learning and the confusion matrix obtained after training. The matrix was used to confirm the accuracy of the scoring of the whole set of mitochondria.

CRediT authorship contribution statement

P.F., M.C.C., and J.J.P. designed the study; P.F. performed experiments; H.P. performed the RNA extraction, Quantitative Real-Time PCR, and mtDNA content experiment; G.B performed fluorescence microscope experiment, V.M and G.B performed optic microscope and area, density and vascular white adipose tissue study, C.M performed technical assistant, C.M performed histological study, P.F., and M.C.C. collected and analyzed data; P.F., H.P,J.P, J.J.P and M.C.C. wrote the manuscript.

Graphical abstract

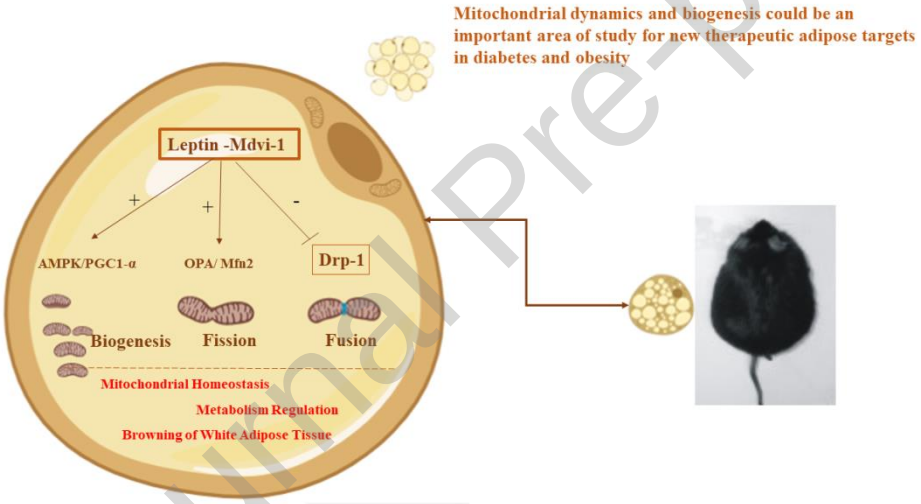

Highlights

- Mitochondrial dynamic and biogenesis are abnormal in white adipose tissue in this animal model of obesity and type 2 diabetes
- Drp-1 fission protein is overexpressed while the fusion- proteins are decreased in this animals
- The Drp-1 blocking with short-term leptin and mdvi-1 treatment improves mitochondrial morphology, fission-to-fusion ratio, activity and metabolism leading the white adipose tissue from beige adipose tissue
- This molecule should be a new therapeutic target for obesity and type 2 diabetes